Review Article

A framework based on spin glass models for the inference of anatomical connectivity from diffusion-weighted MR data – a technical review

J.-F. Mangin,[1]* C. Poupon,[1] Y. Cointepas,[1] D. Rivière,[1] D. Papadopoulos-Orfanos,[1] C. A. Clark,[1] J. Régis[2] and D. Le Bihan[1]

[1]Service Hospitalier Frédéric Joliot, CEA, Orsay, France
[2]Service de Neurochirurgie Fonctionnelle et Stéréotaxique, CHU La Timone, France

ABSTRACT: A family of methods aiming at the reconstruction of a putative fascicle map from any diffusion-weighted dataset is proposed. This fascicle map is defined as a trade-off between local information on voxel microstructure provided by diffusion data and *a priori* information on the low curvature of plausible fascicles. The optimal fascicle map is the minimum energy configuration of a simulated spin glass in which each spin represents a fascicle piece. This spin glass is embedded into a simulated magnetic external field that tends to align the spins along the more probable fiber orientations according to diffusion models. A model of spin interactions related to the curvature of the underlying fascicles introduces a low bending potential constraint. Hence, the optimal configuration is a trade-off between these two kind of forces acting on the spins. Experimental results are presented for the simplest spin glass model made up of compass needles located in the center of each voxel of a tensor based acquisition. Copyright © 2002 John Wiley & Sons, Ltd.

KEYWORDS: diffusion; connectivity; white matter; fiber; regularization; inverse problem; spin glass

INTRODUCTION

A standard computational model of the brain architecture consists of a huge distributed neural network. While the study of the complete topology of this network is far beyond the scope of any experimental method, a better understanding of its general organization at multiple scales may greatly improve the situation of cognitive neurosciences. In the human brain, unfortunately, post-mortem techniques that rely upon the application of tracer molecules to label pathways have significant limitations.[1] Therefore, current knowledge of the large-scale connectivity of the human cerebral cortex is especially sparse,[2] which is a serious handicap for the understanding of fMRI studies. Functional brain mapping aims at highlighting various networks of areas supposed to perform collaborative computations during cognitive tasks.

Diffusion-weighted MRI may turn out to be a powerful tool for the cartography of white matter fiber bundles, which would deeply modify the future of brain mapping. Diffusion MRI gives access to information about the microscopic geometry of biological tissues.[3] Diffusion anisotropy has long been observed in muscle.[4] With the advent of diffusion MRI, anisotropy was also detected *in vivo* at the end of the 1980s in spinal cord[5] and brain white matter.[6,7] While the exact mechanism leading to anisotropic water diffusion in white matter is still not completely clear, water mobility in the fiber direction is greater than in the perpendicular direction.

Hence, more sophisticated acquisition schemes have been devised in order to probe the fiber organization inside MRI voxels. Diffusion tensor imaging (DTI), which is today widely used, was the first attempt to consistently assess the main fiber orientation and other features of tissue microstructure.[8] While this approach has resulted in a lot of interesting applications, it now seems insufficient to elucidate the numerous fiber crossings occurring in cortical gyrus white matter. Therefore, high angular resolution imaging methods have recently been investigated in order to infer a more informative distribution of the water mobility in any direction of space.[9–11] The more sophisticated scheme is diffusion spectrum imaging (DSI), which provides a

*Correspondence to: J.-F. Mangin, Service Hospitalier Frédéric Joliot CEA, 4 place du Général Leclerc, 91401 Orsay Cedex, France. Email: mangin@shfj.cea.fr

distribution of water displacements throughout each voxel.[12] While some work remains to be done to find the optimal trade-off between these 'time expensive' acquisition schemes and the requirements of fiber tracking algorithms, diffusion MRI is now able to provide a reconstructed image of the microscopic geometry for any voxel, which opens the door to great applications.

A number of algorithmic approaches have been recently proposed to study anatomical connectivity from diffusion-weighted data. The general aim is the possibility of asserting which cortical areas or basal ganglia are connected by fascicles of fibers embedded in white matter. For most of these approaches, the putative fascicles are revealed by the step-by-step reconstruction of highest diffusion 3D trajectories.[13–15] The reconstruction is performed from a vector field made up of the local directions of highest diffusion, the diffusion tensor first eigenvector. This class of methods may be related to the computation of fluid streamlines in hydrodynamics.[16] Unfortunately, this approach is not robust to spurious local directions, which induce erroneous forks of the tracking process.[15,17]

Since acquisition artifacts and partial volume averaging generate noisy direction maps, some correction schemes have been designed: tensor Gaussian smoothing,[18] spline-based approximation of the tensor field,[15] vector field anisotropic smoothing,[19] tensor field regularization using partial differential equations,[20] and Markovian regularization.[21,22] This last approach, which embeds the trajectories into the field restoration framework, may be related to another family of tracking methods which do not rely on a vector field but on physics-based propagation ideas. The simplest one is the tensor-line method, which partly overcomes partial volume problems through an advection–diffusion based idea: isotropic or flat tensors do not modify the computed trajectory direction.[23,24] Other methods rely on simulations of a large scale diffusion process throughout white matter, either at the random walks level,[25] or at the macroscopic level using partial differential equation frameworks.[26–28]

The methods mentioned above compute either one trajectory for each given input point (class T),[13–15,23] or a map of connectivity probability for each given input area related for instance to the time of arrival of a simulated large scale propagation process (class P).[25–27] Hence, class P methods are able to detect several areas possibly connected to the input area, while branching is difficult to master with class T methods. A third class (O) of approaches relies on optimization principles leading, for instance, to search for the optimal path between a pair of input points combining diffusion data and path curvature properties.[12] When the goal is the inference of the matrix of connectivity of a set of points, the optimal path approach seems more efficient than class P, which has to compute a connectivity probability map for each point of the set. In return, the connectivity matrix of a set of large areas would be inferred more efficiently by class P.

In this paper, we propose a new family of methods which relies on a global inverse problem framework leading to the definition of optimal solutions. According to the taxonomy introduced above, this family belongs to class O. Compared with the Tuch *et al.* approach,[12] our global methods are searching for the optimal fascicle map interconnecting a set of points sampled on the whole white matter surface. A fascicle map is made up of a set of interconnected fascicle pieces that cover the brain white matter. The fascicles can be automatically reconstructed from this map as paths following the links defined between the fascicle pieces. The fascicle map includes branching locations, which results in more efficiency because the fascicle segments included in several paths are investigated only once during optimization. Once the fascicle map has been inferred, an exhaustive list of pairs of points of the white matter surface linked by a putative fascicle can be provided at low cost. Hence, these methods are more efficient than class P, where a large matrix of connectivity has to be inferred.

The optimality of the fascicle map is defined as a trade-off between local information on voxel microstructure provided by diffusion data and *a priori* information on the low curvature of plausible fascicles. This trade-off is obtained from the minimization of a global measure of the likelihood of a fascicle map knowing the diffusion data set. This likelihood is made up of two kind of terms. The first ones assess the quality of the fit between the local diffusion data and the related local pieces of fascicle. The second ones assess the contextual plausibility of the local configurations of fascicle pieces. Contextual plausibility is used to detect and regularize the spurious fascicle local directions induced by corrupted or ambiguous diffusion data. This measure is modeled using the ideas that most of the fascicles have a rather low bending in anatomical dissections and that a fascicle cannot end up inside white matter. The family of methods built upon this principle can deal in a straightforward way with more or less accurate diffusion data and can embed the possibility of fascicles crossing inside voxels. In the following, the general framework is proposed first. Then, its simplest derivation is described and criticized.

FRAMEWORK

Inverse problem

The reconstruction of the white matter fascicle geometry from diffusion-weighted data may be considered as a standard inverse problem. Like many other inverse problems, fascicle map inference has to deal with acquisition artifacts and coarse data sampling. The

choice of the trade-off between signal-to-noise, spatial and angular resolutions is important relative to the accuracy of the fascicle map that can be reconstructed. If the fascicle map resolution is too high relative to the relevant information included in the data, the inverse problem becomes ill-posed, which means that two different acquisitions of the same brain will yield two very different fascicle maps simply because of noise and partial volume. Any single wrong local diffusion data interpretation may create a spurious fascicle in the map while splitting an actual one. Voxels including crossing fibers are especially difficult to deal with and may lead to different fascicle reconstructions according to the data spatial and angular sampling. It should also be understood that several different local fiber configurations may provide the same diffusion data. For instance, a flat tensor may correspond to a crossing or to a 'fan shaped' fascicle. Hence, there is a need for the problem to be formulated in a way that gives the same unique solution with different acquisitions, at least for the same sampling level.

The MEG/EEG inverse problem is a prototype of very ill-posed problems where a huge number of different source configurations may yield similar data at the sensor level. The main origin of this ill-posedness is the fact that a 3D source configuration has to be inferred from a 2D sparsely sampled surface located outside the brain. The fascicle map inverse problem is less difficult because diffusion MRI provides a spatially dense 3D data set. Hence, this problem is more similar to the fMRI inverse problem where brain neural activity has to be inferred from a spatially dense 3D sampling of hemodynamics. The fact that each corrupted or ill-interpreted local diffusion data results in erroneous local tractography, however, requires a cautious inversion method. Otherwise, untangling white matter fascicle geometry in the cortex vicinity might lead to false conclusions.

A standard approach to deal with ill-posed problems relies on the regularization principle: *a priori* knowledge on the regularity of the most plausible solutions allows the distinction between relevant information and noise. The family of methods proposed in the following uses the reasonable hypothesis that, in case of ambiguity, the most plausible fascicle trajectory is endowed with the lowest curvature. This hypothesis and the additional knowledge that a fascicle should not end inside white matter allows the method to extrapolate the reliable fascicle segments inferred from the areas of unequivocal diffusion data to more problematic white matter areas. A similar idea was previously proposed to restore a road network from very noisy radar satellite images.[29]

Fascicle maps and spin glasses

As mentioned above, the choice of the fascicle map resolution has to be consistent with the amount of relevant information embedded in the diffusion data. For

instance, it seems hopeless to try to recover the trajectories of 100 different fascicles across one given voxel from standard DTI data. While oversampling the trajectory space and using several seed locations in the initial voxel may be appealing to deal with fascicle branching with class T methods, it seems rather difficult to control the result far from the seed. Moreover, when diffusion data are interpolated, additional spurious forks are bound to be created by partial volume effects. Finally, this oversampling strategy might lead some users to misunderstand the diffusion tracts' origin. Diffusion data do not result from a tracer-based methodology that allows axon tracing but on macroscopic measures probing the water diffusion process in voxels crossed by a large number of fibers. Hence, an actual anatomical fascicle has to be made up of thousands of fibers to have a significant influence on diffusion anisotropy. Fortunately, such fascicles made up of a large number of parallel fibers do exist inside white matter, for instance between the retinotopic areas of the visual system. The organization of the fibers inside these fascicles, however, may not be inferred from standard diffusion-data. Hence, the following methods aim at recovering maps including only a limited number of fascicles into each diffusion data voxel.

The first important feature of the fascicle map representation is the volumetric domain of white matter to be reconstructed. In most of our experiments, this domain is simply a mask of the whole white matter. This mask is defined first by a threshold on fractional anisotropy[30] followed by the detection of the largest 3D connected component. Finally the cavities induced by low anisotropy voxels inside white matter are detected as 3D connected components of the mask background and filled. When a high resolution T_1-weighted scan is available, a more accurate white matter mask can be defined provided that EPI spatial distortions are taken into account. Using high-resolution anatomical images provides the assurance that no spurious voxels link two different white matter gyri throughout the separating sulcus.[31]

Once the fascicle map domain has been defined, a representation has to be devised for the local pieces of fascicles. Each piece will have some degrees of freedom, which will lead to set out the inverse problem as an optimization driven issue. While a lot of different approaches may be figured out, we focus in the following on an analogy with spin glasses. Therefore, the pieces of fascicles will be called spins. Whatever the nature of the diffusion data set, it will be embedded into out framework as a non-stationary external magnetic field acting on the spin orientations. The *a priori* knowledge on the fascicle map geometry (low fascicle curvature, no dead ends inside white matter) will be embedded as interactions between neighboring spins.

While our model may be disturbing at first glance because of the potential mix-up with the physical
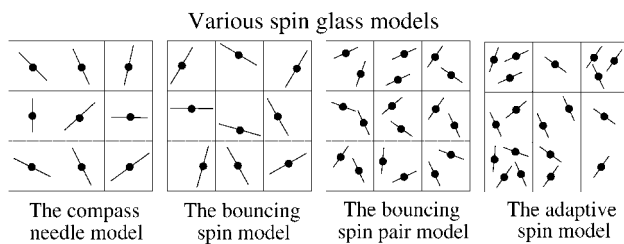
Figure 1. More or less sophisticated spin glass models can be devised. In the compass needle model, spins are located in the voxel center and are endowed with three rotational degrees of freedom. In bouncing spin models, the spins can additionally move inside voxels. In the adaptive model, the number of spins may be chosen according to the nature of the local micro-structure inferred from diffusion data.[11]
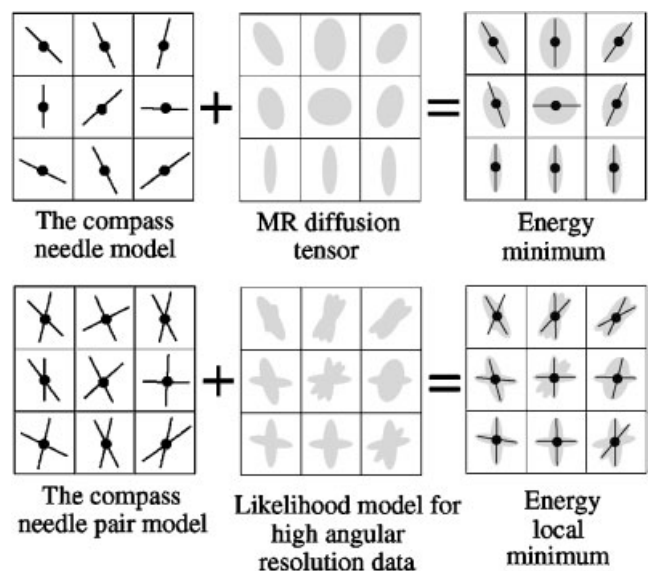

Figure 2. Some spin glasses embedded into a virtual external field stemming from diffusion data. Since no spin interaction occurs, the spins align themselves along directions corresponding to local minima of the likelihood-based potential. With tensor data, the likelihood model is usually built upon the hypothesis that the more plausible fascicle direction corresponds to the highest diffusion. Consequently, the minimal energy configuration corresponds to the field made up of the tensor first eigenvector

processes underlying diffusion MRI acquisition, it should be noted that the simulation of physical phenomena is one of the main sources of inspiration for modern image processing, for instance, the physics of elastic or fluid deformations is used to match brains,[32,33] and various diffusion equations are used to restore images or segment structures.[34] Spin glasses models have been very successful in dealing with complex restoration problems thanks to their good performance relative to stochastic optimization schemes inspired by the simulated annealing principle.[35] The methods described in the following define the solution to the fascicle map inverse problem as the minimal energy configuration of a spin glass. Interestingly, a Bayesian probabilistic interpretation can be provided for this approach: the optimal configuration is the maximal probability realization of a random field.[22]

The white matter domain defined above is discretized in voxels. In the following, these voxels correspond to the diffusion data resolution, but better sampling could be used provided that the diffusion data can be interpolated. The family of methods proposed in this paper includes more or less sophisticated variants related to the kind of spins that live inside the domain voxels (Fig. 1). The simplest model, which has been used during our experiments, puts one compass needle-like spin in the center of each voxel. More advanced models that will be used in the future relax the spin localization in order to improve the fascicle trajectory sampling, or put several spins inside each voxel in order to deal with fascicle crossing.

The external magnetic field models

For each voxel M of the fascicle domain, information on local water mobility inferred from the diffusion data can be used to build models which provide for any direction of space the likelihood of the existence of a crossing fascicle. These models can then be converted into a virtual diffusion based local potential P_D^M acting on the orientations $\vec{v}_i^M$ of the spins i located inside M. Hence, the

virtual potential field made up of these local potentials will act on the simulated spin glass as a non stationary magnetic field. Various likelihood models can be devised according to the nature of the diffusion data. As it stands when using DTI data, these models are directly related to the hypothesis that the diffusion coefficient is greater in the fascicle direction than in neighboring directions. Recent experiments including some higher angular resolution data, however, have proved that this hypothesis is not always true at the level of crossings.[11,36] Hence, a better understanding of the crossing and compartment issues might lead to better likelihood models in the future.[3]

When the spin glass is embedded into such an external potential field, the spin orientations rotate in order to reach a minimum of energy, which can be simulated using a minimization algorithm. Without any spin interaction, a minimum for the whole glass is made up of minima in each voxel. With tensor data, the spins align themselves along the tensor eigenvector associated with the largest eigenvalue (Fig. 2). Hence, the resulting spin glass configuration is equivalent to the vector field used by standard tracking algorithms.[13–15] It should be noted that if a continuous tensor field approximation is used in conjunction with higher spatial resolution or bouncing spin models, the potential P_D^M also depends on the spin localization.

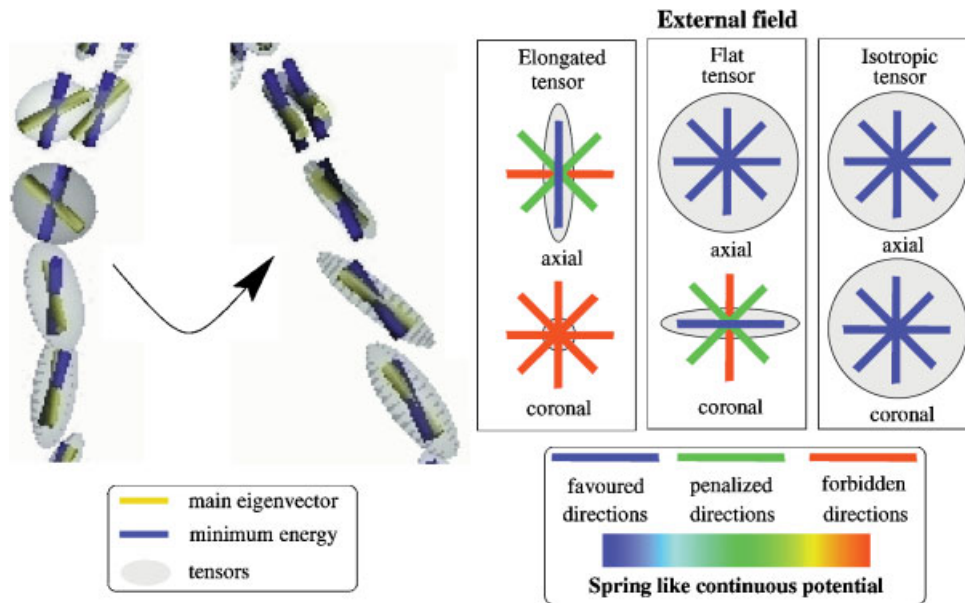In the following, spin interaction potentials are added

Figure 3. Equilibrium found by the spins located into a 'fan-shaped' fascicle. This equilibrium stems from a trade-off between forces acting like springs in order to maintain a high level of diffusion along the spin directions and forces trying to impose alignment with some neighboring spins in order to create a low-curvature fascicle. The largest rotations relative to the direction of highest diffusion occur in the voxels including diverging fibers, resulting in flat tensors.[36] In these voxels the direction of highest diffusion provided by the tensor model is not necessarily related to the fiber orientation

into the glass energy in order to introduce the *a priori* knowledge about the low curvature of most of the fascicles. Hence, spin glass energy minima will correspond to a global trade-off between two different kinds of forces (Fig. 3).

The interaction model

At the resolution of standard diffusion data, the geometry of the fascicle map may be related to the geometry of spaghetti plates, which is illustrated by white matter dissections obtained from Klinger method (Fig. 4). Therefore, the interaction potential that will embed a low curvature constraint for the fascicles is inspired by a simple model of the local bending energy accumulated by spaghetti during cooking, namely a quadratic potential based on the spaghetti local curvature.[22]

Then, a spaghetti potential $P_S^M(i)$ is defined to embed the interactions between each spin i located into voxel M and the neighboring spins, namely the set N_i^M made up of all the other spins located into M and of the spins located in M neighboring voxels in the fascicle map domain. The neighboring spin set N_i^M is split first into forward and backward subsets from the spin i orientation $\vec{v}_i$ (Fig. 7). Then one neighboring spin is selected in each half-neighborhood [respectively $f(i)$ and $b(i)$] in order to create a local fascicle trajectory $b(i)$–i–$f(i)$ endowed with the lowest possible curvature. Note that whatever the

relative orientations of $\vec{v}_{b(i)}$, $\vec{v}_i$ and $\vec{v}_{f(i)}$, a putative fascicle has to be defined because of our assumption that the fascicles cannot lead to dead ends inside white matter. Each time that one half-neighborhood is empty, however, no best point can be defined and the fascicle is supposed to leave white matter. Therefore, no bending constraint is added into $P_S^M(i)$ in that direction.

Whatever the spin glass model (Fig. 1), the lowest

Figure 4. The spaghetti plate-like geometry of white matter illustrated by a brain dissection.[37] The preservation method of Klinger was utilized. Fine forceps (straight or curved) were used to dissect the delicate nerve bundle preparations
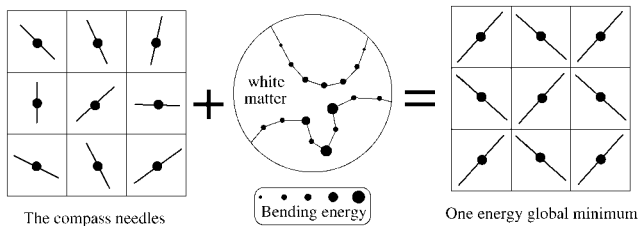
Figure 5. Without external field, the compass needle spin glass subject to bending energy-related interactions leads to straight fascicles

energy configurations induced by the spaghetti interaction potentials are made up of straight fascicles (see Fig. 5). Such configurations, indeed, have a null energy and correspond to spaghetti sets without any cooking. The simplest compass needle model, unfortunately, is biased in some directions by the discrete grid because of the fixed locations of spins. This bias will lead us to relax the spin locations in the near future.

Global energy and minimization

Diffusion based potentials and bending energy based spin interactions are gathered into a global energy E which is defining the solution to the inverse problem as the lowest energy configuration:

$$E = \sum_M \sum_i P_D^M(i) + \alpha \sum_M \sum_i P_S^M(i) \qquad (1)$$

where α is a positive rigidity constant which balances the influence of the *a priori* knowledge on the fascicle low curvature. The solution is obtained using either deterministic or stochastic minimization, according to the quality of the initialization that can be provided.

An important point to be understood is related to the huge number of local minima of the global energy made up only of the sum of $P_S^M(i)$ potentials over the whole fascicle map. A lot of spaghetti plate configurations, indeed, correspond to local minima. This complex energy landscape stems partly from the fact that, once a spaghetti plate has been tangled, it is almost impossible to largely reduce one given spaghetti curvature without increasing the curvature of neighboring ones. This situation means that, without diffusion-based potentials, a deterministic minimization initialized by a random orientation map does not yield a map of straight fascicles.[38] The fascicle map model, however, is more flexible than an actual spaghetti plate because fascicle segments may split and merge during the minimization. Split and merge operations create additional paths throughout the landscape, which greatly reduces the number of local minima. Moreover, adding the diffusion-based potentials to the spin glas energy deeply modifies the landscape. The

diffusion-based potentials select a reduced set of acceptable fascicle map configurations that may explain the diffusion data. Then, the bending energy term allows the minimization to choose among these fascicle maps the one with the smallest curvatures along fascicles.

Fascicle maps and connectivity matrices

In order to resolve connectivity issues, the optimal spin glass has to be converted into a fascicle map, namely a map of fascicle trajectories including some fan-shaped forks (see Fig. 6). In fact, such a fascicle map is implicitly defined for any spin glass configuration during the minimization in order to compute the bending energy of the analogous spaghetti plate. Hence, the optimal fascicle map is directly inferred from the definition of the spin neighbors that minimize bending energy [$f(i)$ and $b(i)$]: a two-way link is created for each [$i, f(i)$] and [$i, b(i)$] pair. The spins endowed with more than two backward or forward links become forks. The spins without backward or forward link lead to gray matter. A straightforward real-time propagation from an input point I provides the list of output points linked to I by a putative fascicle (see Fig. 6). This rapid propagation scheme can be performed for each point leading to grey matter in order to compute an exhaustive sparse matrix of connectivity. The spin potentials may be integrated along each fascicle trajectory in order to assess the connection likelihood.

Because of the huge number of points leading to grey matter, the matrix of connectivity mentioned above is impossible to visualize. Its sparseness, however, allows the design of a compressed representation that will be used to handle brain connectivity in various applications. Anyway, simpler matrices can also be computed when white matter surface points are gathered into subsets corresponding to anatomical or functional divisions.

MATERIALS AND METHOD

In this section, we derive the simplest possible instance of model relying on the previous framework in order to perform a few experiments.

Data acquisition

All scans were acquired on a 1.5 T Signa Horizon Echospeed MRI system (Signa, General Electric Medical Systems, Milwaukee, WI, USA) equipped with magnetic field gradients of up to 22 mT/m^{-1}. A standard quadrature head coil was used for RF transmission and reception of the NMR signal. Head motion was minimized with standard foam padding as provided by the manufacturer. Echo-planar diffusion-weighted images were acquired in
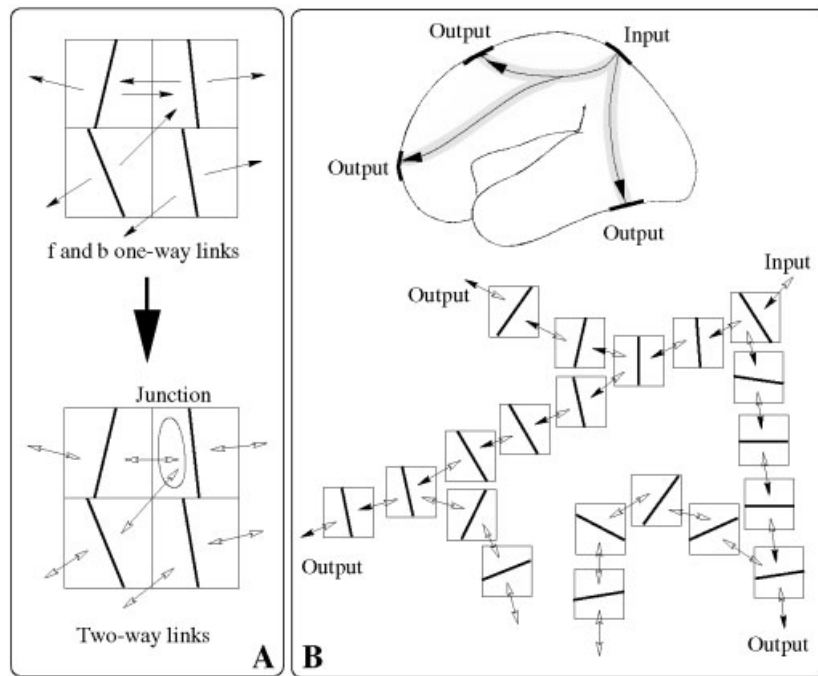
Figure 6. (A) One-way arrows represent the links towards best neighbors. The optimal spin glass is transformed into a fascicle map from a system of two-way links. Some of the spins which have more than one two-way link in the same half neighborhood turn out to be fascicle junctions. (B) Connectivity can be addressed for each input selected into the spin glass. A propagation algorithm follows the links from the input until white matter surface areas are reached. If the propagation comes across a fork, several trajectories may be followed in parallel. The rule which prevents the propagation from proceeding backwards at the level of forks is simple: for each spin the mid-plan has to be crossed before using a new link. Black arrows indicate the links used in the example

the axial plane. Blocks of eight contiguous slices were acquired, each 2.8 mm thick. Seven blocks were acquired covering the entire brain corresponding to 56 slice locations. For each slice location 31 images were acquired; a T_2-weighted image with no diffusion sensitization followed by five diffusion sensitized sets (b values linearly incremented to a maximum value of 1000 s mm^{-2}) in each of six non-collinear directions. These directions were as follows:[39] {(1, 1, 0), (1, 0, 1), (0, 1, 1), (1, −1, 0), (1, 0, −1), (0, 1, −1)}. In order to improve the signal-to-noise ratio this was repeated four times, providing 124 images per slice location. The image resolution was 128×128, field-of-view 24×24 cm, $TE = 84.4$ ms, $TR = 2.5$ s. It should be noted that voxels are anisotropic, which may bias the tracking result. Imaging time excluding time for on-line reconstruction was approximately 37 min. An additional T_1-weighted high resolution 3D dataset was acquired for visualization purposes. A database of nine normal volunteers (men, age range 25–34 years) was acquired with this protocol. All subjects gave informed consent and the study was approved by the local Ethics Committee.

Computation of the diffusion tensor

Before performing the tensor estimation, a mutual information-based unwarping algorithm is applied to the diffusion-weighted dataset to correct for the distortions related to eddy currents induced by the large diffusion sensitizing gradients.[22,40] Following the distortion correction, the diffusion tensor is calculated for each voxel of the brain using the Geman–McLure estimator, which is robust to the presence of outliers in the diffusion-weighted dataset.[22,40]

Derivation of the diffusion-based potential

Using the simple hypothesis that the likelihood of a fascicle local direction is directly related to the diffusion coefficient in that direction, simple expressions can be derived for the diffusion-based potential. For instance, cup-shaped functions built from the discrepancy between the diffusion coefficient in the spin i current direction $d^M(\vec{v}_i^M) = \vec{v}_i^{M'} D^M \vec{v}_i^M$ and the largest diffusion coefficient, namely the largest eigen value of the tensor λ_1^M. While a

lot of variants may be figured out, we have chosen a quadratic expression which leads to an intuitive situation where springs tend to align the spins along the direction of maximal diffusion (see Fig. 3):

$$P_D^M(i) = \left(\frac{\vec{v}_i^{M^t} D^M \vec{v}_i^M - \lambda_1^M}{\|D^M\|} \right)^2 \quad (2)$$

where the tensor norm D^M is normalizing the contribution of voxel M in the complete spin glass energy.[41]

Derivation of the curvature-based potential

In order to define the spin interaction potential as the bending energy of a spaghetti, a discrete analog to the curvature of a continuous line has to be defined as explained in Fig. 7. This 'discrete curvature' is defined for a putative fascicle that links two spins i and j. Hence, a discrete local bending energy can be derived as:

$$e(i,j) = \frac{\max^2[(\vec{v}_i, \vec{u}_{ij}), (\vec{v}_j, \vec{u}_{ij}), (\vec{v}_i, \vec{v}_j)]}{\|\vec{ij}\|} \quad (3)$$

where $\vec{u}_{ij} = \vec{ij}/\|\vec{ij}\|$ is the unitary vector linking i and j, $\vec{v}_i$ is a unitary vector corresponding to the spin i orientation, and $(\vec{V}_1, \vec{V}_2)$ denotes the angle between any pair of vectors $\vec{V}_1$ and $\vec{V}_2$.

Finally, $P_S^M(i)$ is computed as the forward and backward bending energy of a putative fascicle following the $b(i)$–i–$f(i)$ trajectory, where $f(i)$ and $b(i)$ are the forward and backward neighbors which minimize this local bending energy:

$$P_S^M(i) = e[b(i), i] + e[i, f(i)] \quad (4)$$

Global energy and minimization

For the results presented in the following, the weighting α of the bending energy [eqn (1)] has been set to 1 after a study of this parameter influence on the topology of the optimal fascicle map.[22] This *ad hoc* choice, however, may be questioned in the future when actual validation studies will be performed. In the following, results are presented for the compass needle model. The global energy E [eqn (1)] is minimized according to an iterative deterministic scheme which is initialized by the first eigenvector map. The direction space has been discretized in 162 uniformly distributed directions. The spin orientations are iteratively upgraded by the direction that minimizes E. Convergence is reached after about 20 iterations and 30 min of computations. While deterministic minimization provided meaningful results (Fig. 3), simulated annealing will be implemented in the near future in order to untangle fiber crossings with more sophisticated spin glass models (Fig. 1).[29]
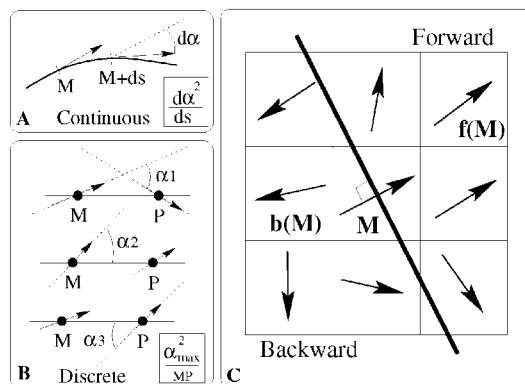

Figure 7. Two-dimensional illustration of the computation of fascicle local bending energy. (A) The spaghetti local bending energy. Note that $c^2 ds = (d\alpha^2/ds) ds = d\alpha^2/ds$ where c denotes local curvature and s curvilinear length. (B) A discrete bending energy is defined between two neighboring spins in order to mimic the continuous case. (C) The neighborhood of each spin $i \in M$ is split in two by a plane orthogonal to $\vec{v}_i^M$ which defines forward and backward neighbors. One point minimizing the discrete bending energy is selected in each of these half-neighborhoods [forwards: $f(i)$, backwards: $b(i)$]. The underlying fascicle is supposed to follow the $b(i)$–i–$f(i)$ trajectory

RESULTS AND DISCUSSION

Some experiments illustrating the positive effect of the low curvature constraints have been proposed elsewhere with simulated data.[38] The fact that these constraints may overcome partial volume-related ambiguities is illustrated in Fig. 3 for a small area of flat tensors located along a pyramidal pathway. A study of the topology of the optimal fascicle map proposed by Poupon *et al.*[22] has shown that the regularization approach highly reduces the number of dead ends inside white matter and restores the somatotopic organization of large bundles into parallel fascicles. In this paper, we focus on results highlighting the weaknesses of the current approach based on the compass needle model and on tensor data to explain the need for more sophisticated spin glass models and high angular resolution acquisition schemes. We then propose a comparison with the closest alternative tracking approaches. Finally, we make the link with another research project that aims at a systematic division of the cortex into gyri[42] in order to infer a matrix of connectivity whose scale is similar to the matrices obtained for some animal species from architectonic divisions.[2]

Fan shaped trajectories

In order to study the potential of the method for the reconstruction of fan-shaped fascicle trajectories, several input points have been selected at different
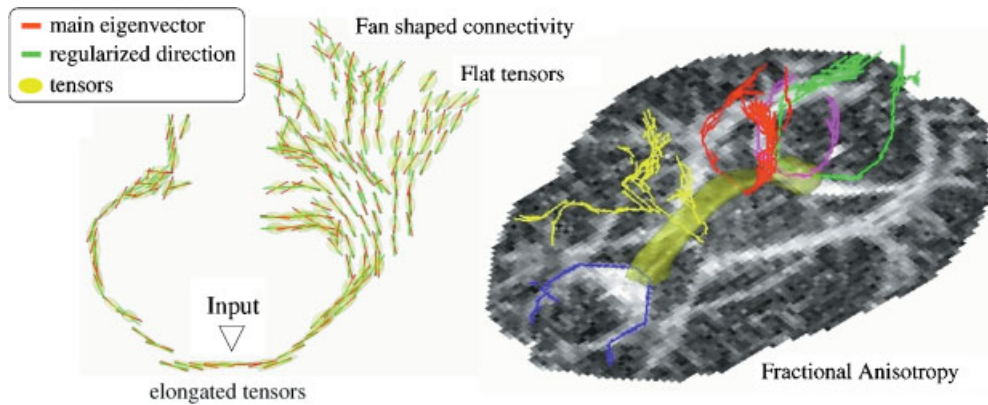
Figure 8. Left: the usual double fan shaped result obtained for an input located into corpus callosum. Right: several tracking results illustrating that most of the putative fascicles reach the cortex medial face, while actual fascicles supposed to reach the cortex external faces are usually lost because of the existence of large areas of crossings.[36]

locations into the corpus callosum. Propagation has been applied in both directions. Some of the results are presented in Fig. 8. Most of the tracked trajectories show a similar pattern. In the neighborhood of the input point, the high anisotropy of the tensors located in the corpus callosum leads to a simple fascicle segment without any fork. Forks become more and more numerous as the trajectories near the cortex, however, where a lot of flat tensors can be observed. Hence, the set of trajectories obtained from a given input looks like a double fan, which could be expected for a set of commisural fibers densely compacted into one corpus callosum voxel. The fact that most of the fan outputs reach the medial faces of the cortex, however, highlights one of the weaknesses of the compass needle model: since only one spin is allowed into each voxel, most of the actual commissural fascicles supposed to reach the cortex external faces are lost at the level of the crossings with ascending and longitudinal pathways. This observation calls for the use of the more advanced spin glass models proposed in Fig. 1.

Large areas of flat tensors

In order to illustrate further the problems induced by large areas of ambiguous tensors, a tracking result from an input point located into brain stem is provided (Fig. 9). The main trajectory is crossing a large area of flat tensors bound to be related to the crossing of two large bundles.[36] Since the compass needle model is endowed with only one spin per voxel, one of the bundles wins the competition related to the energy driving the glass. Hence, the fascicles of the other bundle are not reconstructed. While using several spins per voxel may partly overcome the problem, a better angular resolution is required for the diffusion data in order to simplify the minimization problems. Otherwise, it may turn out to be

very difficult to find the paths reconnecting the fascicle segments located on both sides of the crossing area. Furthermore, with tensor data, the spin glass energy global minimum may not yield the actual anatomical configuration.

Global versus individual path optimization

A basic difference between our global approach and other approaches intending to regularize the standard stream-
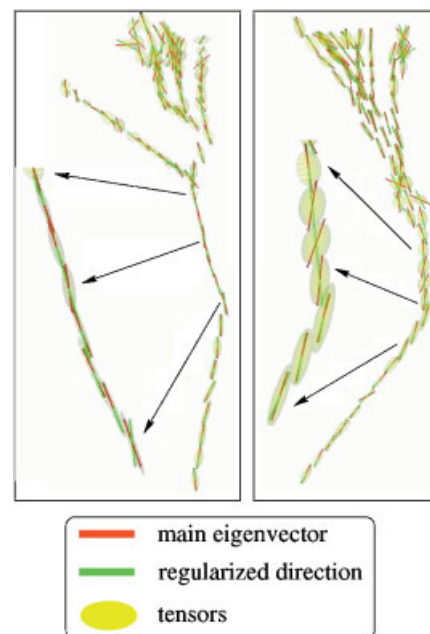

Figure 9. In large crossing areas, the bundle inducing the highest diffusion direction is masking the crossing fascicles. Without highest angular resolution data, this configuration seems very difficult to untangle

line approach, namely the tensorlines[23,24] and the path-by-path approach proposed by Tuch *et al.*,[12] is the competition between neighboring trajectories. The global optimization gives the system a larger field of view when an ambiguous area has to be untangled. While this is supposed to improve the result for large ambiguous areas, this has still to be proven and will certainly require more sophisticated spin models.

Another important difference between our global approach to the fascicle map inverse problem and the path-by-path approach proposed by Tuch *et al.* is related to the fact that the spin glass approach cannot provide a probability of connection for any pair of points. The fascicle map, indeed, includes only the more plausible fascicles. Hence, the matrix of connection probabilities provided by the spin glas method is a sparse thresholded version of the dense matrices that could be computed from the path-by-path approach or from a large set of whole-brain propagations.[27] This observation raises several complex issues.

How much interesting information is lost by this thresholding effect? This point is related to the potentially ill-posed nature of the inverse problem mentioned above. The spin glass threshold is imposed by the number of spins that are in the glass. Increasing the number of spins will increase the number of recon-structed fascicles and reduce the sparseness of the connectivity matrix. According to the above discussion, the compass needle model is too poor to recover all the information provided by the diffusion data. Increasing the number of spins, however, will not lead to a dense connectivity matrix but to a limit sparse matrix that includes all the connections that are made up by a large number of fibers.

Although the missing part of the matrix may be interesting because it could include some clues on the connections induced by smaller fascicles diverging from the main ones, we think this additional information may be computed during a second algorithmic stage. It should be noted that the path-by-path approach is relatively ineffective when a large connectivity matrix has to be inferred, because most of the computed optimal paths do not correspond to actual fascicles. Tracer-based methods have shown that the actual connectivy matrices are highly sparse.[2] Moreover, the individual optimal path problem may turn out to be computationally difficult because of local minima. This kind of problem has usually been tackled using propagation-like algorithms stemming from graph theory that may be related to class P approaches. From this point of view, the simulated annealing approach mentioned in Tuch *et al.* abstract may not be robust and requires further explanations.[12]

One of the requirements to obtain a good performance of actual implementations of simulated annealing is related to the nature of the energy lanscape. Spin glasses, whose physical properties have inspired this stochastic
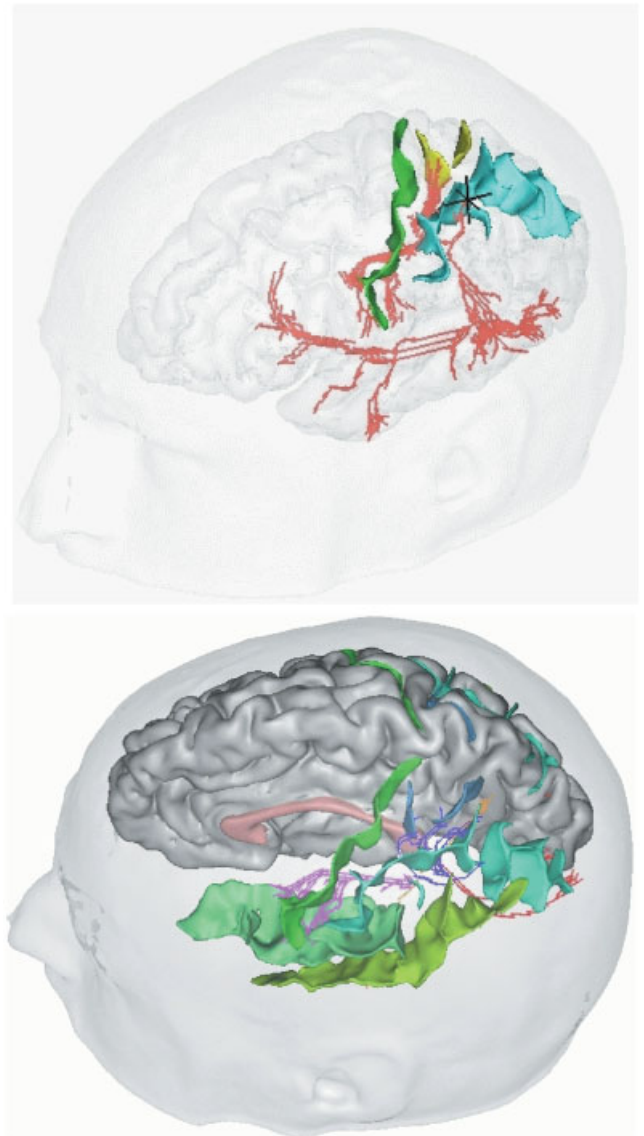

Figure 10. Top: an input located into inferior parietal lobule has led to a distributed set of outputs located into parietal, temporal and frontal areas (red, putative fascicles; green, central sulcus; yellow, superior postcentral sulcus; blue, interparietal fissure). Bottom: a subdivision of the cortical surface according to the automatic recognition of the main sulci will be used to sort the various fascicles linking cortical gyri in order to infer a cortex connectivity matrix (green, various sulci; blue, pink and yellow, intra-hemispheric associative fascicles; red, commissural fascicles)

optimization idea, usually lead to one large valley full of shallow local minima. Hence, escaping from such local minima requires few additional energy and short sequences of configuration modifications to get over potential barriers. In contrast, the landscape associated to paths with two fixed extremities may be more hilly. Hence the simulated annealing behavior may be highly dependent on the allowed path deformations during the optimization and on the path initialization, which may

require some simplified propagation-like approach to get, for instance, the shortest path. It is important to understand that the flexibility of the spin glass approach during optimization is related to the split and merge like behavior of small fascicle segments made up of a few spins, while a deformable path would behave like an actual indivisible spaghetti. If one part of the spaghetti is located in a wrong valley, it is very difficult to make it cross the ridge leading to the other branch of the diffusion-based fork. More details on the Tuch *et al.* method are required to discuss that point further.

Towards connectivity matrices

Although many improvements should stem from the new spin glass models suggested in this paper, the current fascicle maps can be used to perform first studies of cortico-cortical connectivity. Inputs located at the cortex level already yield rich sets of connected outputs (Fig. 10). While a very interesting application consists of assessing the connectivity matrices of sets of individual functional activations,[14] few areas of the cortical surface can be exhaustively divided from current fMRI studies like the visual system.[43] Therefore, we have launched a research project which aims to provide a road map of the large-scale anatomical connectivity of cortical gyri. Such a map could be compared with the current knowledge of distributed cognitive systems inferred from different domains of neurosciences. Moreover, this map could be endowed with statistical information in order to open the door to population comparisons.

This project implies the systematic division of the cortical surface into a set of gyri that will be used as the connectivity matrix input. In order to overcome the tedious manual gyrus delineation, a virtual system expert of cortical anatomy has been designed.[42] This system segments and labels automatically the main cortical sulci from a standard T_1-weighted MR scan. This expert has been trained on a set of 25 manually labeled brains in order to learn the huge inter-individual variability of the cortical folding patterns.[44] This sulcus labeling can be used further to split the cortical surface into gyri defined by several limiting sulci using geodesic distance-based Voronoï diagrams.[31] Hence, the numerous putative U-fascicles passing under the sulci will be sorted according to the locations of their extremities in order to fill a gyrus connectivity matrix (Fig. 10).

While elongated gyri will have to be split into several pieces in order to improve the map spatial resolution, we hope that a better understanding of the cortical folding process will allow finer anatomical subdivisions according to a map of the sulcus primal sketches observed in MR antenatal images.[45] This sulcal root map[46] may be deeply related to the underlying fascicle geometry according to the tension-based mechanism proposed as one explication to the folding morphogenesis.[47]

Validations

The comparison of the various algorithmic methods that have been proposed for diffusion-based tractography will require an important validation effort which will rapidly become a full research program. While the more attractive approach, at first glance, is the cumbersome animal-based comparison with tracer methods, many other research directions could provide interesting information about the algorithm behaviors whatever the potential problems related to actual diffusion data. Hence, the building up of an open database of simulated diffusion data related to known geometries is now urgent.[15,24] Another very attractive kind of data is related to phantoms made up of various fiber geometries.[10] Finally, the stability of computed connectivity matrices across individuals would be a good validation, even if we have very few information about the interindividual variability of the cortex connectivity.

CONCLUSION

In this paper, we have formalized the reconstruction of a putative fascicle map from diffusion-weighted data as a global inverse problem. The proposed framework is flexible enough to be adapted to foreseeable evolutions of MR acquisition schemes. In our opinion, the inverse problem point of view will help to clarify what reliable information can be extracted from a diffusion-weighted dataset. More and more informative connectivity matrices will be computed from the reconstructed fascicle maps, leading to a very attractive new field of research for neurosciences, ranging from pure graph theory to brain growth or new insights into connectivity-related pathologies. For instance, we plan to rapidly infer a road map of the large-scale connectivity of brain gyri that will be correlated with maps of cognitive systems inferred from fMRI.

REFERENCES

1. Rye DB. Tracking neural pathways with MRI. *Trends Neurosci.* 1999; **22**(9): 373–374.
2. Young MP, Scannell JW, Burns G. The Analysis of Cortical Connectivity. Neuroscience Intelligence Unit. Springer: Berlin, 1995.
3. Le Bihan D, Mangin J-F, Poupon C, Clark CA, Pappata S, Molko N, Chabriat H. Diffusion tensor imaging: concepts and applications. *J. Magn. Reson. Imag.* 2001; **13**: 534–546.
4. Cleveland GG, Chang DC, Hazelwood CF. Nuclear magnetic resonance measurements of skeletal muscle. anisotropy of the diffusion coefficient of the intracellular water. *Biophys. J.* 1976; **16**: 1043–1053.
5. Moseley ME, Cohen Y, Kucharczyk J. Diffusion-weighted MR imaging of anisotropic water diffusion in cat central nervous system. *Radiology* 1990; **176**: 439–446.
6. Chenevert TL, Brunberg JA, Pipe JG. Anisotropic diffusion within human white matter: demonstration with NMR techniques in vivo. *Radiology* 1990; **177**: 401–405.

7. Turner R, Le Bihan D, Maier J, Vavrek R, Hedges LK, Pekar J. Echo-planar imaging of intravoxel incoherent motions. *Radiology* 1990; **177**: 407–414.

8. Basser PJ, Mattiello J, LeBihan D. MR diffusion tensor spectroscopy and imaging. *Biophys. J.* 1994; **66**: 259–267.

9. Tuch DS, Weisskoff RM, Belliveau JW, Wedeen VJ. High angular resolution diffusion imaging of the human brain. In *VIIth ISMRM*, Philadelphia, USA, 1999.

10. Von dem Hagen E, Henkelman RM. Orientational diffusion reflects fiber structure within a voxel. In *ISMRM-ESMRMB*, Glasgow, 2001; 1528.

11. Frank L. Characterization of anisotropy in high angular resolution diffusion weighted MRI. In *ISMRM-ESMRMB*, Glasgow, 2001; 1531.

12. Tuch DS, Wiegell MR, Reese TG, Belliveau JW, Van Wedeen J. Measuring corticocortical connectivity matrices with diffusion spectrum imaging. In *ISMRM-ESMRMB*, Glasgow, 2001; 502.

13. Mori S, Crain BJ, Chacko VP, Van Zijl PCM. Three dimensional tracking of axonal projections in the brain by magnetic resonance imaging. *Ann. Neurol.* 1999; **45**: 265–269.

14. Conturo TE, Lori NF, Cull TS, Akbudak E, Snyder AZ, Shimony JS, McKinstry RC, Burton H, Raichle ME. Tracking neuronal fiber pathways in the living human brain. *Proc. Natl Acad. Sci. USA* 1999; **96**: 10422–10427.

15. Basser PJ, Pajevic S, Pierpaoli C, Duda J, Aldroubi A. In vivo fiber tractography using DT-MRI data. *Magn. Reson. Med.* 2000; **44**(4): 625–632.

16. Yeung P, Pope S. An algorithm for tracking fluid particles in numerical simulations of homogeneous turbulence. *J. Comput. Phys.* 1988; **79**: 373–416.

17. Pierpaoli C, Barnett AS, Pajevic S, Virta A, Basser PJ. Validation of DT-MRI tractography in the descending motor pathways of human subjects. In *ISMRM-ESMRMB*, Glasgow, 2001; 501.

18. Westin C-F, Maier SE, Khidir B, Everett P, Jolesz FA, Kikinis R. Image processing for diffusion tensor magnetic resonance imaging. In MICCAI'99, Cambridge, UK, LNCS-1679. Springer: Berlin, 1999; 441–452.

19. Coulon O, Alexander DC, Arridge SR. A regularization scheme for diffusion tensor magnetic resonance images. In *XVIIth IPMI*, NCS-2082. Springer: Berlin, 2001; 92–105.

20. Tschumperle D, Deriche R. Diffusion tensor regularization with constraints preservation. In *CVPR.*, Hawai, 2001.

21. Poupon C, Mangin J-F, Frouin V, Régis J, Poupon F, Pachot-Clouard M, Le Bihan D, Bloch I. Regularization of MR diffusion tensor maps for tracking brain white matter bundles. In MICCAI'98, MIT, LNCS-1496. Springer: Berlin, 1998; 489–498.

22. Poupon C, Clark CA, Frouin V, Régis J, Bloch I, Le Bihan D, Mangin J-F. Regularization of diffusion-based direction maps for the tracking of brain white matter fascicles. *NeuroImage* 2000; **12**: 184–195.

23. Weinstein D, Kindlmann G, Lundberg E. Tensorlines: advection-diffusion based propagation through diffusion tensor fields. In IEEE Visualization. IEEE: New York, 1999; 249.

24. Lazar M, Alexander A. Error analysis of white matter tracking algorithms (streamlines and tensorlines) for DT-MRI. In *ISMRM-ESMRMB*, Glasgow, 2001; 506.

25. Koch M, Norris DG, Hund-Georgiadis M. An investigation of functional and anatomical connectivity using diffusion tensor imaging. In *ISMRM-ESMRMB*, Glasgow, 2001; 1509.

26. Gembris D, Schumacher H, Suter D. Solving the diffusion equation for fiber tracking in the living human brain. In *ISMRM-ESMRMB*, Glasgow, 2001; 1529.

27. Parker GJM, Wheeler-Kingssbott CA, Barker GJ. Distributed anatomical brain connectivity derived from diffusion tensor imaging. In *XVIIth IPMI*, LNCS-2082. Springer: Berlin, 2001; 106–120.

28. Batchelor PG, Hill DLG, Calamante F, Atkinson D. Study of connectivity in the brain using the full diffusion tensor from MRI. In XVIIth IPMI, LNCS-2082. Springer: Berlin, 2001; 121–133.

29. Tupin F, Maitre H, Mangin J-F, Nicholas J-M, Pechersky E. Detection of linear features in SAR images: application to the road network extraction. *IEEE Geosci. Remote Sens.* 1998; **36**(2): 434–453.

30. Pierpaoli C, Basser PJ. Toward a quantitative assessment of diffusion anisotropy. *Magn. Reson. Mag.* 1996; **36**: 893–906.

31. Mangin J-F, Frouin V, Bloch I, Regis J, Lopez-Krahe J. From 3D magnetic resonance images to structural representations of the cortex topography using topology preserving deformations. *J. Math. Imag. Vision* 1995; **5**(4): 297–318.

32. Bajcsy R, Kovacic R. Multiresolution elastic matching. *Comput. Vision Graph. Image Process.* 1989; **46**: 1–21.

33. Miller MI, Christensen GE, amit Y, Grenander U. Mathematical textbook of deformable neuroanatomies. *Proc. Natl Acad. Sci. USA* 1993; **90**(24): 11944–11948.

34. Perona P, Malik J. Scale-space and edge detection using anisotropic diffusion. *IEEE Trans. Pattern Anal. Mach. Intell.* 1990; **12**(7): 629–639.

35. Geman S, Geman D. Stochastic relaxation. Gibbs distributions, and the Bayesian restoration of images. *IEEE Trans. Pattern Anal. Mach. Intell.* 1984; **6**(6): 721–741.

36. Wiegell MR, Larsson HB, Wedeen VJ. Fiber crossing in human brain depicted with diffusion tensor MR imaging. *Radiology* 2000; **217**(3): 897–903.

37. Williams TH, Gluhbegovic N, Jew JY. The human brain: dissections of the real brain. Virtual Hospital, University of Iowa; www.vh.org/Providers/Textbooks/BrainAnatomy, 1997.

38. Poupon C, Mangin J-F, Clark CA, Frouin V, Régis J, Le Bihan D, Bloch I. Towards inference of human brain connectivity from MR diffusion tensor data. *Med. Image Anal.* 2001; **5**: 1–15.

39. Pierpaoli C, Jezzard P, Basser PJ, Barnett A, Di Chiro G. Diffusion tensor MR imaging of the human brain. *Radiology* 1996; **201**: 637–648.

40. Mangin J-F, Poupon C, Clark C, Le Bihan D, Bloch I. Eddy-current distortion correction and robust tensor estimation for MR diffusion imaging. In MICCAI'01, Utrecht, LNCS. Springer: Berlin, 2001; 186–194.

41. Basser PJ, Pierpaoli C. Microstructural and physiological features of tissues elucidated by quantitative-diffusion-tensor MRI. *J. Magn. Reson.* 1996; **111**: 209–219.

42. Rivière D, Mangin J-F, Papadopoulos D, Martinez J-M, Frouin V, Régis J. Automatic recognition of cortical sulci using a congregation of neural networks. In MICCAI, Pittsburgh, LNCS 1935. Springer: Berlin, 2000; 40–49.

43. Tootel R, Dale A, Sereno M, Malach R. New images from human visual cortex. *Trends Neurosci.* 1996; **19**: 481–489.

44. Ono M, Kubik S, Abernathey CD. Atlas of the Cerebral Sulci. Thieme: Germany, 1990.

45. Cachia A, Mangin J-F, Boddaert N, Régis J, Kherif F, Sonigo P, Zilbovicius M, Bloch I, Brunelle F. Study of cortical folding process with prenatal MR imaging. In ISMRM-ESMRMB, Glasgow. 2001; 121.

46. Régis J, Mangin J-F, Frouin V, Sastre F, Peragut JC, Samson Y. Generic model for the localization of the cerebral cortex and preoperative multimodal integration in epilepsy surgery. *Stereotact. Funct. Neurosurg.* 1995; **65**: 72–80.

47. Van Essen DC. A tension-based theory of morphogenesis and compact wiring in the central nervous system. *Nature* 1997; **385**: 313–318.